Modeling Earth Systems and Environment
https://doi.org/10.1007/s40808-023-01782-7

ORIGINAL ARTICLE

A preliminary geophysical investigation of lead mineralization in parts of the crystalline basement complex of Nigeria

Leke Sunday Adebiyi[1,2] · Akinola Bolaji Eluwole[2] · Akindeji Opeyemi Fajana[2] · Naheem Banji Salawu[2,3]

Received: 10 March 2023 / Accepted: 16 April 2023

Abstract

The present study investigated crustal structures and geological bodies in parts of the crystalline basement of Nigeria using high-resolution airborne magnetic data and a Very Low-Frequency Electromagnetic survey. The purpose is to provide preliminary insight into the lead mineralization identified for the first time in parts of the crystalline basement, as well as to find new promising areas for follow-up mineral investigations. Aeromagnetic anomaly data were interpreted across the study area using standard geophysical techniques consisting of horizontal gradient magnitude, pseudo-gravity transformation and source parameter imaging. The horizontal gradient magnitude anomalies reveal a considerable component of the studied area hosting the lead mineralization. The pseudo-gravity transformation identified a few northwest-southeast geological features which are characterized by high pseudo-gravity anomalies and surrounded on both sides by linear low anomalies that signify a structural deformation. The source parameter imaging shows more closely the geological formation hosting a known lead mining site. To precisely map the extension and trend of the lead mineralization within the geological formation, five very low-frequency electromagnetic survey profiles were established in a northeast-southwest direction covering parts of the geological formation. The results showed northeast and north-northeast extensions of the lead mineralization within the geological formation. Our overall assessment demonstrates the integration of magnetic and Very Low-Frequency Electromagnetic methods as powerful tools for mapping lead deposits.

Keywords Aeromagnetic anomaly · Geological formation · Lead pit · Basement complex

Introduction

Lead was discovered in Nigeria in the 1950s when it was first attributed to a magmatic emplacement of mafic igneous intrusions in the Nigerian rift basin known as the Benue trough (Farrington 1952; Olade and Morton 1985). However, subsequent studies found that the origin of lead in the trough was more hydrothermal than magmatic (Offodile 1980; Olade and Morton 1985; Akande and Mücke 1989, 1993; Maurin and Benkhelil 1990; Oha et al. 2017; Adebiyi et al. 2020). The studies equally identified an association with minor to significant amounts of zinc, copper, baryte and silver, where they occur as lodes filling fractures within the sedimentary sequence (Farrington 1952; Offodile 1980; Olade and Morton 1985; Akande and Mücke 1989; Maurin and Benkhelil 1990; Oha et al. 2017). Since the discovery of lead in Nigeria, it has been widely assumed that it can only be found in the Benue trough (Olade and Morton 1985; Akande and Mücke 1989; Oha et al. 2017). However, we recently identified the metal in parts of the Nigerian basement complex which is underlain primarily by crystalline rocks. This, nevertheless, contradicts the widespread belief that lead mineralization in Nigeria is restricted to the Benue trough. To pave the way for a rigorous geological mapping, we carried out a preliminary geophysical investigation to identify any regional tectonic structure that may be associated with the mineralization and also to outline possible extensions of the metal beyond the current mining location. A geophysical investigation consisting of high-resolution airborne magnetic and Very Low-Frequency Electromagnetic (VLF-EM) methods was deployed. The magnetic

✉ Leke Sunday Adebiyi
adebiyi.leke@lmu.edu.ng; olalakes2012@gmail.com

[1] Department of Physical Sciences, Landmark University, Kwara State, PMB 1001, Omu-Aran, Nigeria

[2] Department of Geophysics, Federal University, Oye-Ekiti, Nigeria

[3] BS Geophysical and Consultancy Ltd, Ilorin, Nigeria

Published online: 04 May 2023

method was used because of its effectiveness in delineating geological structures such as fractures and boundaries of different rock formations (Nabighian et al. 2005). The VLF-EM method, on the other hand, was chosen because of its capability to precisely identify metallic deposits where they are trapped within fractures or rock boundaries (Sharma et al. 2014; Upadhyay et al. 2020).

Location and geological setting

The study area falls mainly within Kwara State in west-central Nigeria, while a small part fall in Niger State in north-central Nigeria. The study area is underlain mainly by the reactivated Archaean basement rocks comprising the migmatite-gneisses, orthogneisses, paragneisses, fragments of silicified quartzite-schist belts, and Pan-African granitoid. An abridged geological map adapted from (Thiéblemont et al. 2018) shows the study area to be intersected by the F3 splits of the Anka-Yauri-Iseyin (AYI) shear zone (Fig. 1a) whereas the geological map of Kwara State by the Nigerian Geological Survey Agency shows detailed geological information of the study area (Fig. 1b) (NGSA 2006). The geological map of the study area, derived from the geological map of Kwara State, shows the shear zone area to be underlain mainly by quartzite rock whereas the mining area is shown to be underlain by migmatite rock (Fig. 1c). The regional fracture cutting through the study area exhibits mainly NNE-SSW structural alignment (Adepelumi et al. 2008; Awoyemi et al. 2017; Adebiyi et al. 2022).

Data and methods

Magnetic data

High-resolution aeromagnetic anomaly data of the study area were acquired and analysed. The acquisition of the data was done by Fugro Airborne Survey for the Nigerian government. The survey orientation was NW–SE at a mean barometric flight altitude of roughly 80 m. The data were acquired at a regular profile spacing of 500 m and tied at every 2000 m (Reford et al. 2010). Essential corrections and data improvements were implemented by Fugro Airborne. The data were griddled at 100 m spacing utilizing the Minimum Curvature technique (Briggs 1974) and shown as a 2-D

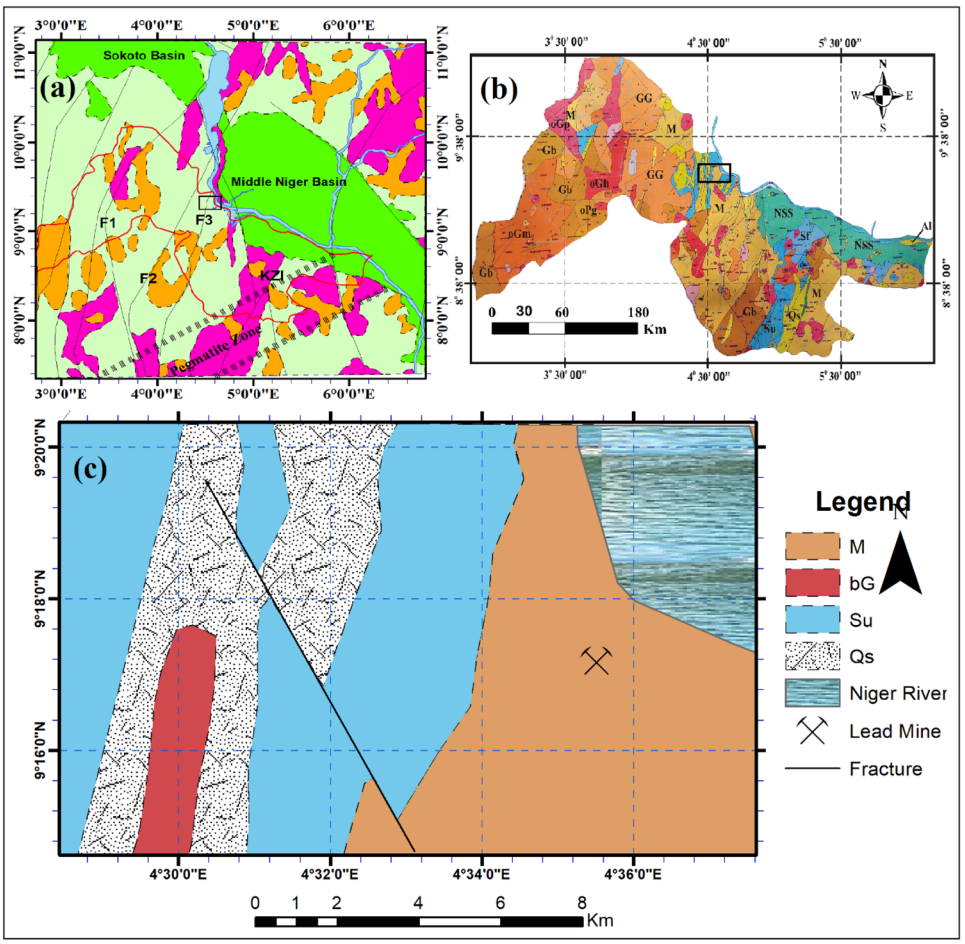

Fig. 1 **a** Abridged geological map showing two splits of the AYI shear zone (Thiéblemont et al. 2018) **b** Detailed geological map of Kwara State (NGSA 2006) **c** Geological map of study area showing the artisanal lead pit in part of Kwara State (NGSA 2006)

map of residual magnetic intensity (Fig. 2). The artisanal mining pit in the area was geolocated on the aeromagnetic anomaly map. Similarly. the Anka-Yauri-Iseyin (AYI) shear zone was inferred from discontinuities in the aeromagnetic anomalies in sheared fault area. This allowed us to estimate the distance between the artisanal mining pit and the shear zone. The estimated distance is 7.8 km. The Niger River was equally geolocated on the aeromagnetic anomaly map and is approximately 1.7 km east of the mining pit.

Magnetic methods

Magnetic methods are mathematical tools or models used for analysing magnetic data (Nabighian et al. 2005). In this study, the aeromagnetic anomaly data of the study area was analysed using magnetic methods such as horizontal gradient magnitude (HGM), pseudo gravity transformation (PGT), and source parameter imaging (SPI). The methods were effectively utilized to show the location, depth and orientation of various geological features underlining the studied area. The magnetic methods used in this study are as follows:

Horizontal gradient magnitude

Horizontal gradient magnitude (HGM) is one of the mathematical models for interpreting magnetic data (Phillips 2000). Because the amplitude of a yet to be interpreted magnetic data is not always centred on the edges of the causal body, it is difficult to delineate with certainty the location or boundary of the causal body (Thurston and Brown 1994; Blakely 1995; Phillips 2000; Beamish 2016). However, when the HGM model is used, the data amplitude systematically align with the edges of the causal body enabling the description of the location and boundary of the causal body (Phillips 2000; Beamish 2016). In terms of resolution, HGM method has the highest resolution among all the edge detection methods (Pilkington and Tschirhart 2017). The method, nevertheless, is sensitive to the direction of the inducing magnetic field and the dip of the causal body (Verduzco et al. 2004; Pilkington 2007). The dependence of the method on the magnetization direction, however, can be reduced by subjecting the original data to a mathematical model known as a reduction to the magnetic equator or most importantly the pseudo-gravity transformation analysis (Baranov 1957; Verduzco et al. 2004; Panepinto et al. 2014; Mashhadi and Safari 2020). The expression for the HGM model for gridded magnetic data is shown in Eq. 1.

$$|HGM(x,y)| = \sqrt{\left(\frac{\partial F}{\partial x}\right)^2 + \left(\frac{\partial F}{\partial y}\right)^2} \quad (1)$$

where $\frac{\partial F}{\partial x}$ and $\frac{\partial F}{\partial y}$ are the first-order partial derivatives of the residual magnetic intensity field F in x and y horizontal directions respectively. Further details of the HGM are available in the published work of (Blakely and Simpson 1986; Thurston and Brown 1994). In this study, the HGM model was implemented on the reduced to-magnetic equator

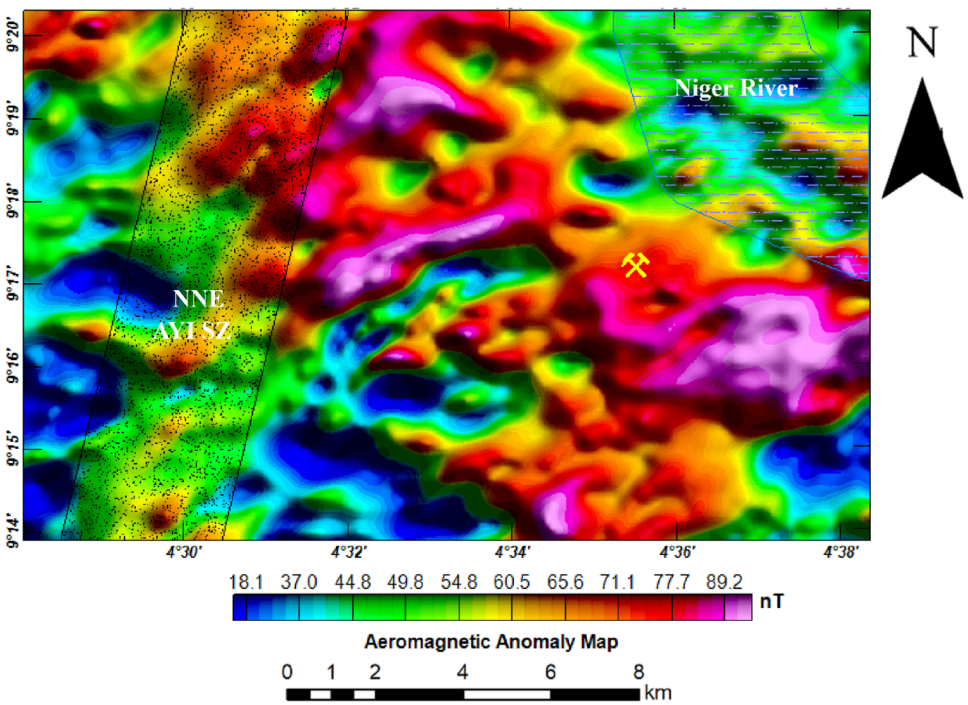

Fig. 2 Aeromagnetic anomaly map of the study area showing the location of the artisanal mining pit and the boundary of the shear zone through the study area

airborne magnetic data and also on the pseudo-gravity anomaly map to reveal the locations and structural alignments of magnetic source bodies.

Pseudo gravity transformation

A pseudo-gravity is an assumed gravity anomaly observable when a magnetization contrast is replaced by an equivalence density contrast (Baranov 1957; Murthy 1969; Bilim and Ates 2004; Panepinto et al. 2014; Mashhadi and Safari 2020). Due to the dipolar nature of magnetic sources and the fact that the magnetization of a body can point in any direction, magnetic responses are far more complicated than gravitational ones. Luckily, pseudo-gravity transformation is an anomaly simplifier, making the analysis of magnetic data considerably simpler. Pseudo-gravity transformation possesses fascinating features that reduce the stronger effect of shallow magnetic sources and increase the dominance of magnetic anomalies from deeper sources. The relationship between the magnetic potential and gravitational field established by Poisson leads to the pseudo-gravity transformation (Blakely 1995; Panepinto et al. 2014). The magnetic and gravitational scalar potentials of a body with uniform magnetization and density in volume v are given by Eqs. 2 and 3 respectively (Baranov 1957; Panepinto et al. 2014)

$$V(q) = -M\nabla_q \iiint_V \frac{1}{r} dv \tag{2}$$

$$U(q) = G\rho \iiint_V \frac{1}{r} dv \tag{3}$$

where q is the data observation point, r is the source distance, M is the magnetization distribution, G is the gravitational constant and ρ the source density. Using Eqs. 2 and 3 we obtained Eqs. 4, 5 and 6

$$V(q) = -\frac{1}{G\rho} M\nabla_q U \tag{4}$$

where $g_M = \nabla_q U$ (5)

$$V(q) = -\frac{1}{G\rho} M g_M \tag{6}$$

From Poisson's relation, g_M refers to the component of gravity in the magnetization direction. The pseudo-gravity operator converts the magnetic anomaly into a gravity-like response as if the body's magnetism were replaced with the same density distribution, where density and magnetic susceptibility have a perfect linear association (Baranov 1957; Blakely 1995; Panepinto et al. 2014). The pseudo-gravity transformation was applied to the aeromagnetic anomaly data in the current study area to locate deep-seated geological bodies.

Source parameter imaging analysis

The source parameter imaging (SPI) model was developed by (Smith et al. 1998). The model is based on a complex analytic signal that computes source parameters from gridded aeromagnetic data. It is also referred to as the local wavenumber technique. This method estimates depths over isolated contacts without making assumptions about the source thickness (Smith et al. 1998). Edge positions, depths, dips, and susceptibility contrasts are all displayed on SPI solution grids. The local wavenumber map is more similar to geology than the original magnetic map or its derivatives (Thurston and Brown 1994; Smith et al. 1998; Salako 2014). To estimate the depth values using the source parameter imaging (SPI) model, the local wavenumber in Eq. 7 is used (Thurston and Smith 1997; Smith et al. 1998).

$$K = \frac{\frac{\partial^2 F}{\partial x \partial z}\frac{\partial F}{\partial x} + \frac{\partial^2 F}{\partial y \partial z}\frac{\partial F}{\partial y} + \frac{\partial^2 F}{\partial z^2}\frac{\partial F}{\partial z}}{\left(\frac{\partial F}{\partial x}\right)^2 + \left(\frac{\partial F}{\partial y}\right)^2 + \left(\frac{\partial F}{\partial z}\right)^2} \tag{7}$$

where K_{max} is the maximum value of the local wavenumber (K) above the step-type source body. The depth estimates are thus calculated using the reciprocal of the local wavenumber given in Eq. 8.

$$Depth_{x=0} = \frac{1}{K_{\max}} \tag{8}$$

The SPI model was used to delineate the boundary and depth of the geological formation suspected to host the lead.

Very low-frequency electromagnetic (VLF-EM) method

A high-powered military radio transmitter operating in the frequency range of 5 to 30 kHz generates the VLF-EM signal (Gürer et al. 2009; Sharma et al. 2014). The signal propagation is vertical at first, but over long distances, it becomes horizontal, allowing it to penetrate the earth and induce secondary electromagnetic fields in subsurface conductors (Sharma and Baranwal 2005; Sharma et al. 2014; Zakaria et al. 2021). The induced fields have two components—the in-phase and out-of-phase which are the real and imaginary components respectively. The goal of the VLF-EM surveys is the acquisition of the in-phase and out-of-phase components. The data acquired are thus subjected to further analysis to identify the location and depth of the causal bodies. Two well-established mathematical models are often used for this purpose, they are the Fraser and Karous-Hjelt

filtering techniques. Equations 9 and 10 show the models for the Fraser and Karous-Hjelt filters respectively (Fraser 1969; Karous and Hjelt 1983). The raw data are shifted by 90^0 as a result of the filtering, so that the crossover and inflexion points become peaks centred on the causal bodies (Reynolds 1997; Bosch and Müller 2001). The Karous-Hjelt filter generates two-dimensional subsurface sections to visualise the position and depth of the causal bodies (Karous and Hjelt 1983; Bosch and Müller 2001).

$$F_i = \left(D_{i+2} + D_{i+3}\right) - \left(D_i + D_{i+1}\right) \tag{9}$$

$$F_i = 0.102D_i - 0.059D_{i+1} + 0.561D_{i+2} - 0.561D_{i+4} + 0.059D_{i+5} - 0.102D_{i+6} \tag{10}$$

where D represents each data and i stands for the serial number of each data beginning from 1, 2, 3, 4,……..n.

In the study area, we established five VLF-EM profiles in a northeast-southwest direction over the geological formation to determine the extent and orientation of the lead mineralization. The data were acquired with the aid of an ABEM WADI VLF-EM device. The coordinates of the data points were simultaneously acquired using a handheld GPS device. Figure 3 shows the layout of the VLF-EM survey in the studied area.

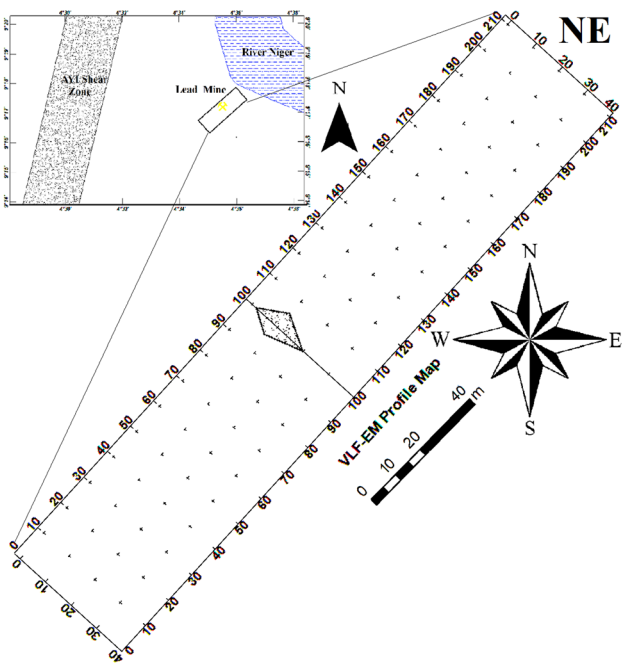

Fig. 3 Base map showing the VLF-Em profiles and the artisanal mining pit

Results and discussion

Detection of source edges

Horizontal gradient magnitude anomaly map

The high-resolution airborne magnetic data of the studied area was first reduced to the magnetic equator and the HGM magnetic model was applied. The purpose of reducing the original data to the magnetic equator was to reduce the effect of the inclination and declination on the HGM analysis. The result obtained shows a significant number of shallow-seated geologic bodies and linear structures underlining the studied area (Fig. 4). The HGM map shows the orientation and boundaries of the north-northeast trending AYI shear zone to the west of the mining area. The map equally identified with the high amplitude of the HGM analysis a few northeast trending structures while the mining area is located within the low amplitude of the HGM map (Fig. 4). The distance of the lead mining pit from the AYI shear zone as we have earlier measured is 7.8 km. Considering this great distance, we could not have possibly linked the lead mineralization to the shear zone. Nevertheless, a few northwest-trending structural alignments are evident in the HGM analysis, particularly in parts of the study area covered by the Niger River. Although the HGM analysis revealed the structural alignments of many shallow-seated geological features, it could not reveal the deep-seated geological features throughout the study area since the analysis is only sensitive to shallow-seated geological features.

Pseudo-gravity transformation anomaly map

To reveal regional deep-seated geological features which are not visible in the HGM analysis in Fig. 4, we applied a pseudo-gravity transformation (PGT) to the aeromagnetic anomaly map. The PGT, as an integral method, possesses a unique ability to suppress shallow geologic features while enhancing deep-seated regional features. The PGT analysis reveals, in addition to the already established structural alignments, new northwest-trending regional features that extend from the mining area to the Niger River area (Fig. 5). The mining pit is shown on the PGT map (Fig. 5) to be located in a part of the study area defined by low gravity anomalies that indicate an association with magnetically quiet geological formation. Consequently, the pseudo-gravity analysis suggests a link between lead mineralization and the northwest-trending geological feature. The pseudo-gravity transformation results in this study are highly significant as it reveals the geodynamic nature of the tectonic events in the studied area.

Furthermore, we applied HGM analysis on the PGT map (Fig. 6) to further reveal the edges of northwest-trending

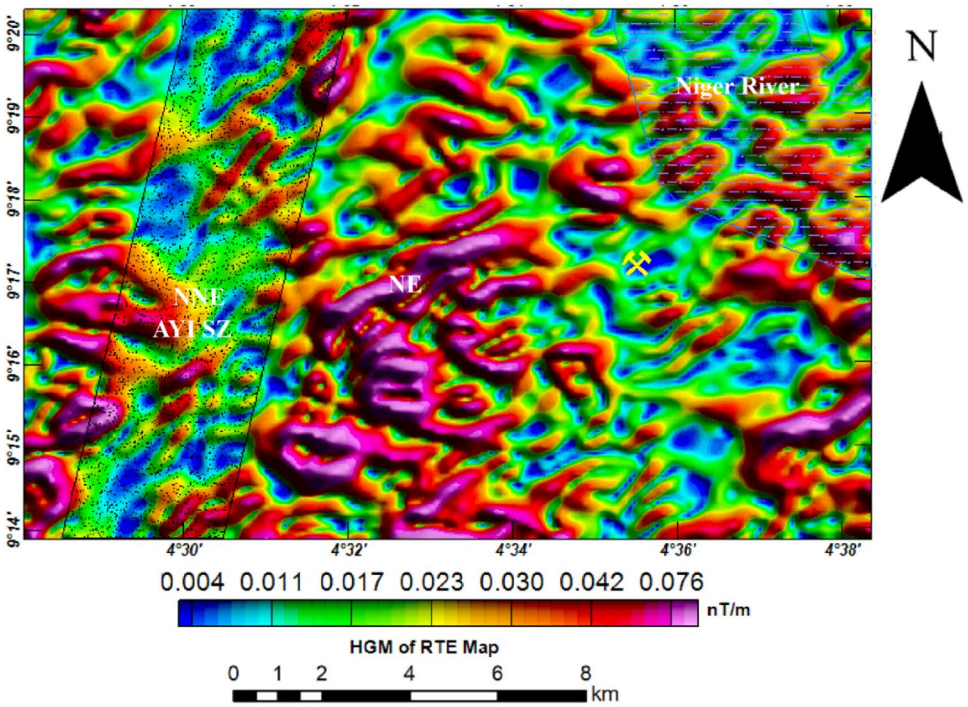

Fig. 4 Horizontal gradient magnitude (HGM) aeromagnetic anomaly map of the study area

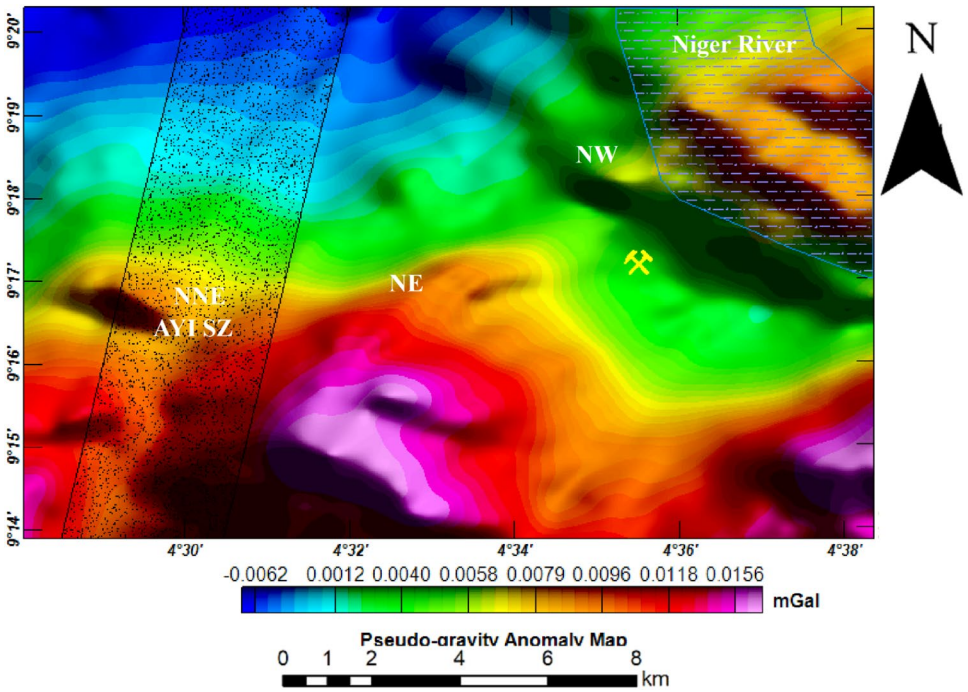

Fig. 5 Colour-shaded pseudo-gravity anomaly map of the study area

regional features that were not clearly shown in the original HGM map (see Fig. 4). The new HGM result (Fig. 6) shows the mining area within the low amplitude of the HGM. The map further reveals the northwest-trending structural alignment as well as the north-northeast trending AYI shear zone. The region around the mining location and the parts occupied by the Niger River show positive prospects for large-scale lead exploitations.

Source parameter imaging map

The SPI analysis was used to complement the HGM technique since it is capable of delineating precisely dipping and

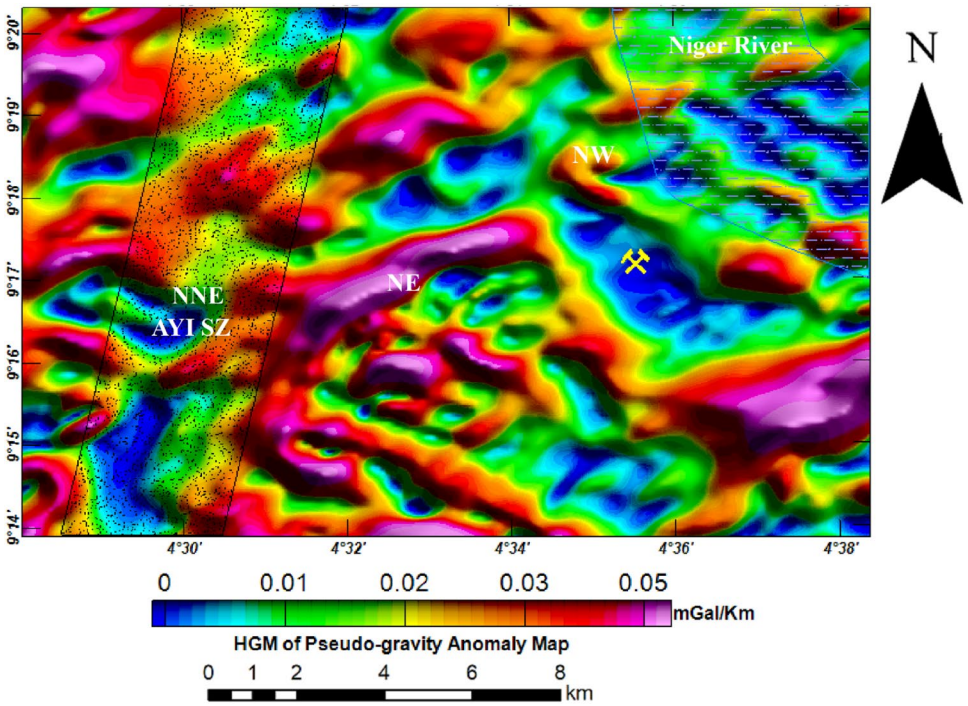

Fig. 6 Horizontal gradient magnitude of the pseudo-gravity anomaly map

non-dipping contacts. The SPI estimated the locations and depths of shallow, fairly deep, and deep magnetic sources, allowing for ground follow-up (Fig. 7). The shallow sources are less than 100 m deep, whereas the fairly deep and deep sources are more than 100 m deep. The AYI shear zone has a large area of deep-seated magnetic sources, though the southern and northern parts have mostly shallow magnetic sources. The mining area, on the other hand, has shallow and fairly deep sources. We identified from the SPI analysis a distinct geological formation hosting the artisanal mining pit. The length and width of the said geological formation are roughly 2300 m and 670 m respectively. We, therefore, concentrated our efforts on shallow sources because the

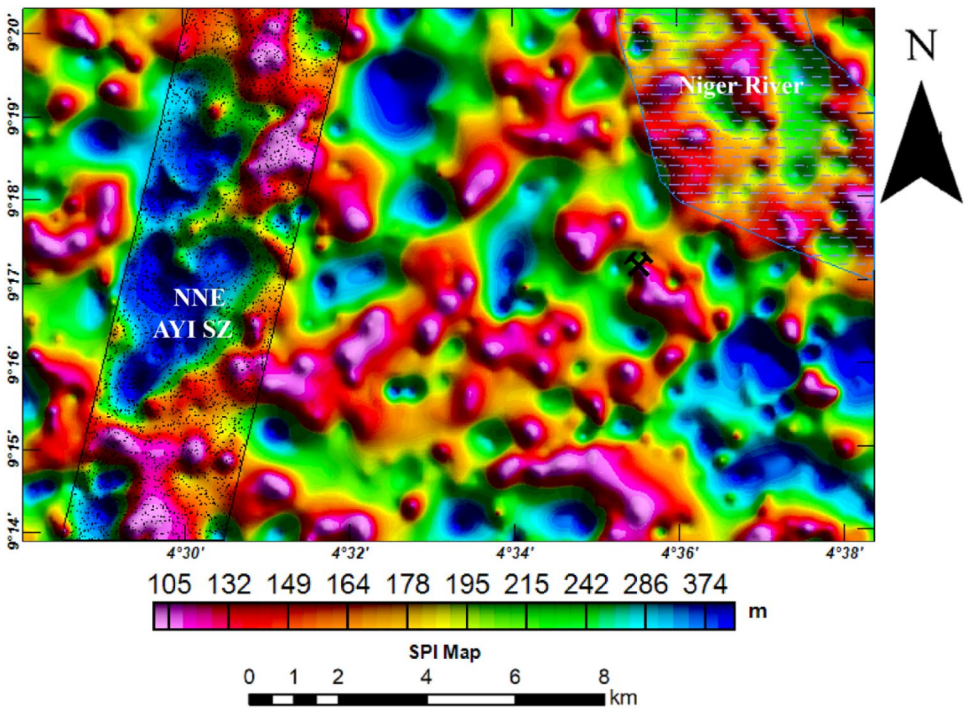

Fig. 7 Depth distribution for magnetic sources derived from SPI interpretation

Lead exploration in the artisanal mining pit begins at barely 10 m deep.

Very-low frequency electromagnetic results

The Fraser and Karous-Hjelt filters were used to analyse the VLF-EM data. The filters were applied to in-phase data acquired along the five VLF-EM profiles. The Fraser filter results had peaks that coincided with the high conductivity areas of the Karous-Hjelt 2-D sections (Fig. 8). These high conductivity zones are considered to be weak zones with distinctive VLF-EM signatures emanating from the subsurface conductor, such as fractures or ore bodies (Michael et al. 2013). The depth to the tops of the conductive causal bodies is 10 m (Fig. 8a, b and c), which matched well with the depth measured in the mining pit (Fig. 9). The results indicate the possibility of depths greater than 30 m below the subsurface. The VLF-EM filtered data were gridded to create a VLF map of the survey area (Fig. 10). The map shows a few conductive zones with a conductivity scale well over 7.9. The mining pit in the study area is located within one of the conductive zones (Fig. 10), indicating that the conductive zones are potential

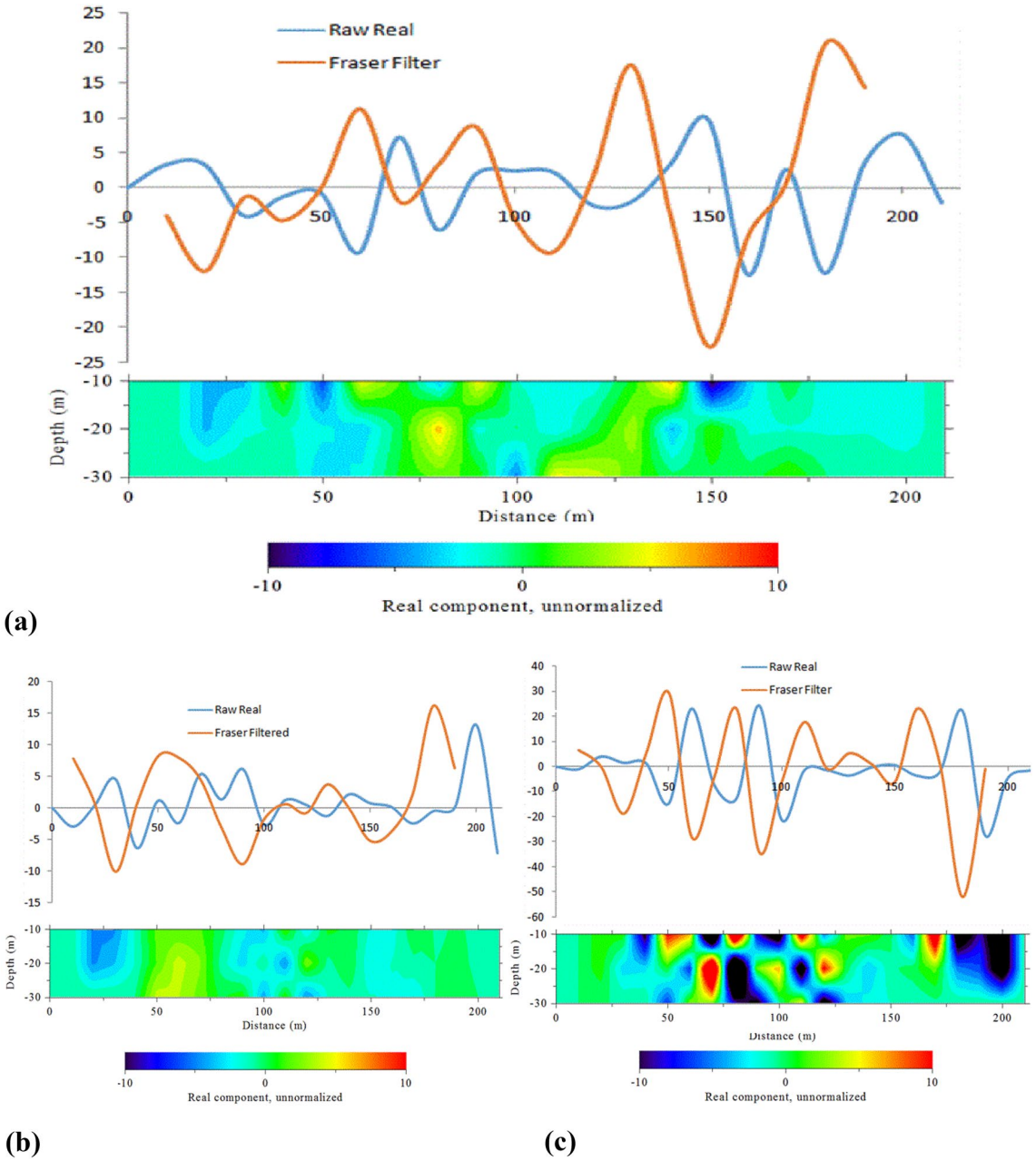

Fig. 8 Fraser and Karous-Hjelt results for **a** Profile 1 **b** Profile 3 **c** Profile 5

Fig. 9 Snapshot of the **a** opened mining pit taken from inside the pit **b** mining area covered by younger sediments

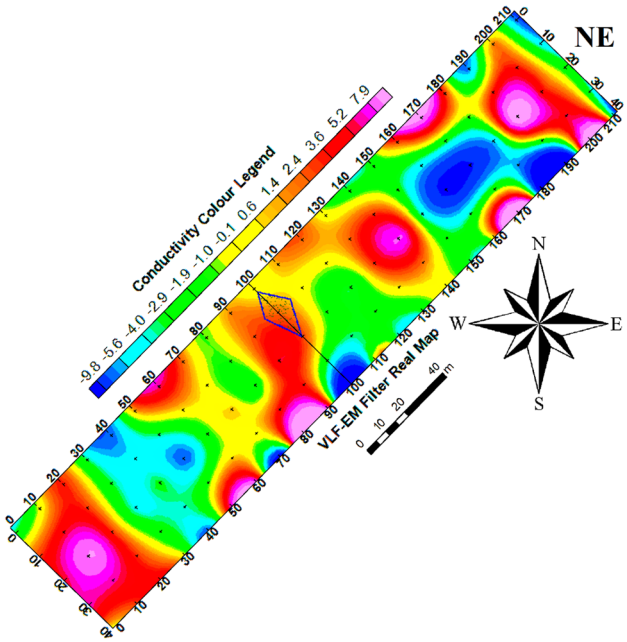

Fig. 10 VLF-EM Filtered Real map showing lead mineral targets

areas for focusing lead exploitation in the study area. The strikes of the conductive zones are mainly NW–SE and NNW-SSE. The widths vary from 10 to 30 m (Fig. 10). The VLF-EM results show a possibility for substantial lead mineralization beyond the current mining location.

Conclusion

The study of lead mineralization in parts of the crystalline basement complex of Nigeria shows that the mineralization has a positive prospect for large-scale exploitation. The magnetic methods highlighted a few northwest-southeast geological structures that could be related to lead mineralization. Similarly, the methods provided an estimation of the locations and depth of the geological formation suspected of hosting the lead, thereby allowing us to focus the ground geophysical survey on specific targets. Furthermore, the VLF-EM survey revealed the location, strike and depth of the lead within the geological formation. The results showed the lead mineralization to have mainly NW–SE and NNW-SSE geological strikes. The width of the mineralized formations varies from 10 to 30 m, while the depth to the top of the deposits is 10 m and appears to extend more than 30 m below the surface. Finally, the NW–SE crustal deformation in the airborne magnetic data analysis is suspected to have a tight control on lead mineralization. Finally, a follow-up geological investigation is recommended to provide insights into the origin of lead mineralization in the studied area.

Declarations

Conflict of interest The authors declare that they have no known competing financial interests or personal relationships that could appear to have influenced the work reported in this paper.

References

Adebiyi LS, Fatoba JO, Salawu NB et al (2020) Analysis of aeromagnetic data: application to early-late cretaceous events in parts of Lower Benue trough, Southern Nigeria. J Appl Geophy. https://doi.org/10.1016/j.jappgeo.2020.104052

Adebiyi LS, Eluwole AB, Salawu NB et al (2022) A new insight into the structural framework of a crystalline formation and the

adjoining sedimentary terrain in parts of the precambrian basement complex of Nigeria. Pure Appl Geophys 179:1749–1773. https://doi.org/10.1007/s00024-022-02994-1

Adepelumi AA, Ako BD, Ajayi TR et al (2008) Integrated geophysical mapping of the Ifewara transcurrent fault system, Nigeria. J Afr Earth Sc 52:161–166. https://doi.org/10.1016/j.jafrearsci.2008.07.002

Akande SO, Mücke A (1989) Mineralogical, textural and paragenetic studies of the leadzinccopper mineralization in the lower Benue Trough (Nigeria) and their genetic implications. J Afr Earth Sc 9:23–29. https://doi.org/10.1016/0899-5362(89)90004-3

Akande SO, Mücke A (1993) Coexisting copper sulphides and sulphosalts in the Abakaliki Pb-Zn deposit, lower Benue Trough (Nigeria) and their genetic significance. Mineral Petrol 47:183–192. https://doi.org/10.1007/BF01161566

Awoyemi MO, Hammed OS, Falade SC et al (2017) Geophysical investigation of the possible extension of Ifewara fault zone beyond Ilesa area, southwestern Nigeria. Arab J Geosci 10:1–14. https://doi.org/10.1007/s12517-016-2813-z

Baranov V (1957) A new method for interpretation of aeromagnetic maps: pseudo-gravimetric anomalies. Geophysics 22:359–382. https://doi.org/10.1190/1.1438369

Beamish D (2016) Enhancing the resolution of airborne gamma-ray data using horizontal gradients. J Appl Geophy. https://doi.org/10.1016/j.jappgeo.2016.07.006

Bilim F, Ates A (2004) An enhanced method for estimation of body magnetization direction from pseudogravity and gravity data. Comput Geosci. https://doi.org/10.1016/j.cageo.2003.09.003

Blakely RJ (1995) Potential theory in gravity and magnetic applications. Potential theory in gravity and magnetic applications. Cambridge University Press, Cambridge. https://doi.org/10.1017/CBO9780511549816

Blakely RJ, Simpson RW (1986) Approximating edges of source bodies from magnetic or gravity anomalies. Geophysics 51. https://doi.org/10.1190/1.1442197

Bosch FP, Müller I (2001) Continuous gradient VLF measurements: a new possibility for high resolution mapping of karst structures. First Break 19:343–350. https://doi.org/10.1046/J.1365-2397.2001.00173.X

Briggs IC (1974) Machine contouring using minimum curvature. Geophysics 39:39–48. https://doi.org/10.1190/1.1440410

Farrington JL (1952) A preliminary description of the Nigerian lead-zinc field. Econ Geol. https://doi.org/10.2113/gsecongeo.47.6.583

Fraser DC (1969) Contouring of VLF-EM data. Geophysics 34. https://doi.org/10.1190/1.1440065

Gürer A, Bayrak M, Gürer ÖF (2009) A VLF survey using current gathering phenomena for tracing buried faults of Fethiye-Burdur Fault Zone, Turkey. J Appl Geophy. https://doi.org/10.1016/j.jappgeo.2009.03.011

Karous M, Hjelt SE (1983) Linear filtering of VLF dip-angle measurements. Geophys Prospect. https://doi.org/10.1111/j.1365-2478.1983.tb01085.x

Mashhadi SR, Safari M (2020) The effectiveness of pseudo-gravity transformation in mineral exploration: an example from a placer magnetite deposit. 3rd Conference on Geophysics for Mineral Exploration and Mining, Held at Near Surface Geoscience 2020. https://doi.org/10.3997/2214-4609.202020015

Maurin JC, Benkhelil J (1990) Model of Pb/Zn mineralization genesis in the Cretaceous Benue Trough (Nigeria): structural, geophysical and geochemical constraints. J Afr Earth Sc 11:345–349. https://doi.org/10.1016/0899-5362(90)90013-5

Michael GA, Agwul AA, Akam OD (2013) Fracture zone detection using very low frequency (VLF) electromagnetic method in parts of Oban Massif, southeastern Nigeria. Pelagia Res Libr Adv Appl Sci Res 4

Murthy IVR (1969) Interpretation of gravity anomalies of dykes by pseudo-magnetic transformation. Pure Appl Geophys PAGEOPH 73:43–46. https://doi.org/10.1007/BF00875120

Nabighian MN, Grauch VJS, Hansen RO, et al (2005) The historical development of the magnetic method in exploration. Geophysics. https://doi.org/10.1190/1.2133784

Nigerian Geological Survey Agency (2006) Nationwide Geological Map. NGSA, Nigeria

Offodile ME (1980) A mineral survey of the Cretaceous of the Benue Valley, Nigeria. Cretac Res. https://doi.org/10.1016/0195-6671(80)90020-8

Oha IA, Onuoha KM, Dada SS (2017) Contrasting styles of lead-zinc-barium mineralization in the Lower Benue Trough Southeastern Nigeria. Earth Sci Res J 21:7. https://doi.org/10.15446/esrj.v21n1.39703

Olade MA, Morton RD (1985) Origin of lead-zinc mineralization in the southern Benue Trough, Nigeria—Fluid inclusion and trace element studies. Miner Depos 20:76–80. https://doi.org/10.1007/BF00204313

Panepinto S, De Luca L, Mantovani M et al (2014) Using the pseudo-gravity functional transform to enhance deep-magnetic sources and enrich regional gravity data. SEG Tech Progr Expand Abstr 33:1275–1279. https://doi.org/10.1190/segam2014-1323.1

Phillips JD (2000) Locating magnetic contacts: a comparison of the horizontal gradient, analytic signal, and local wavenumber methods. 2000 SEG Annual Meeting. Soc Explor Geophys 19:402–405. https://doi.org/10.1190/1.1816078

Pilkington M (2007) Locating geologic contacts with magnitude transforms of magnetic data. J Appl Geophy. https://doi.org/10.1016/j.jappgeo.2007.06.001

Pilkington M, Tschirhart V (2017) Practical considerations in the use of edge detectors for geologic mapping using magnetic data. Geophysics. https://doi.org/10.1190/GEO2016-0364.1

Reford SW, James Misener D, Ugalde HA et al (2010) Nigeria's nationwide high-resolution airborne geophysical surveys. Society of Exploration Geophysicists International Exposition and 80th Annual Meeting 2010. SEG 2010:1835–1839. https://doi.org/10.1190/1.3513199

Reynolds JM (1997) An introduction to applied and environmental geophysics. https://doi.org/10.1071/pvv2011n155other

Salako KA (2014) Depth to basement determination using source parameter imaging (SPI) of aeromagnetic data : an application to upper Benue Trough and Borno Basin, Northeast, Nigeria. Acad Res Int 5:74–86

Sharma SP, Baranwal VC (2005) Delineation of groundwater-bearing fracture zones in a hard rock area integrating very low frequency electromagnetic and resistivity data. J Appl Geophy. https://doi.org/10.1016/j.jappgeo.2004.10.003

Sharma SP, Biswas A, Baranwal VC (2014) Very low-frequency electromagnetic method: a shallow subsurface investigation technique for geophysical applications recent trends. In: Modelling of environmental contaminants. Springer, New Delhi

Smith RS, Thurston JB, Dai TF, MacLeod IN (1998) iSPI™—the improved source parameter imaging method. Geophys Prospect 46:141–151. https://doi.org/10.1046/j.1365-2478.1998.00084.x

Thiéblemont D, Callec Y, Fernandez-Alonso M, Chène F (2018) A geological and isotopic framework of precambrian terrains in Western Central Africa: an introduction. Springer International Publishing, Cham, pp 107–132. https://doi.org/10.1007/978-3-319-68920-3_5

Thurston JB, Brown RJ (1994) Automated source-edge location with a new variable pass-band horizontal-gradient operator. Geophysics. https://doi.org/10.1190/1.1443615

Thurston JB, Smith RS (1997) Automatic conversion of magnetic data to depth, dip, and susceptibility contrast using the SPI (TM) method. Geophysics 62:807–813. https://doi.org/10.1190/1.1444190

Upadhyay A, Singh A, Panda KP, Sharma SP (2020) Delineation of gold mineralization near Lawa village, North Singhbhum Mobile Belt, India, using electrical resistivity imaging, self-potential and very low frequency methods. J Appl Geophy. https://doi.org/10.1016/j.jappgeo.2019.103902

Verduzco B, Fairhead JD, Green CM, MacKenzie C (2004) New insights into magnetic derivatives for structural mapping. Leading Edge 23:116–119. https://doi.org/10.1190/1.1651454

Zakaria MF, Kusumayudha SB, Pratistho B et al (2021) Application of very low frequency (VLF) method for estimating karst underground river in Tanjungsari District. RSF Conf Series Eng Technol. https://doi.org/10.31098/cset.v1i1.423

Terms and Conditions

Springer Nature journal content, brought to you courtesy of Springer Nature Customer Service Center GmbH (“Springer Nature”).
Springer Nature supports a reasonable amount of sharing of research papers by authors, subscribers and authorised users (“Users”), for small-scale personal, non-commercial use provided that all copyright, trade and service marks and other proprietary notices are maintained. By accessing, sharing, receiving or otherwise using the Springer Nature journal content you agree to these terms of use (“Terms”). For these purposes, Springer Nature considers academic use (by researchers and students) to be non-commercial.
These Terms are supplementary and will apply in addition to any applicable website terms and conditions, a relevant site licence or a personal subscription. These Terms will prevail over any conflict or ambiguity with regards to the relevant terms, a site licence or a personal subscription (to the extent of the conflict or ambiguity only). For Creative Commons-licensed articles, the terms of the Creative Commons license used will apply.
We collect and use personal data to provide access to the Springer Nature journal content. We may also use these personal data internally within ResearchGate and Springer Nature and as agreed share it, in an anonymised way, for purposes of tracking, analysis and reporting. We will not otherwise disclose your personal data outside the ResearchGate or the Springer Nature group of companies unless we have your permission as detailed in the Privacy Policy.
While Users may use the Springer Nature journal content for small scale, personal non-commercial use, it is important to note that Users may not:

1. use such content for the purpose of providing other users with access on a regular or large scale basis or as a means to circumvent access control;
2. use such content where to do so would be considered a criminal or statutory offence in any jurisdiction, or gives rise to civil liability, or is otherwise unlawful;
3. falsely or misleadingly imply or suggest endorsement, approval , sponsorship, or association unless explicitly agreed to by Springer Nature in writing;
4. use bots or other automated methods to access the content or redirect messages
5. override any security feature or exclusionary protocol; or
6. share the content in order to create substitute for Springer Nature products or services or a systematic database of Springer Nature journal content.

In line with the restriction against commercial use, Springer Nature does not permit the creation of a product or service that creates revenue, royalties, rent or income from our content or its inclusion as part of a paid for service or for other commercial gain. Springer Nature journal content cannot be used for inter-library loans and librarians may not upload Springer Nature journal content on a large scale into their, or any other, institutional repository.
These terms of use are reviewed regularly and may be amended at any time. Springer Nature is not obligated to publish any information or content on this website and may remove it or features or functionality at our sole discretion, at any time with or without notice. Springer Nature may revoke this licence to you at any time and remove access to any copies of the Springer Nature journal content which have been saved.
To the fullest extent permitted by law, Springer Nature makes no warranties, representations or guarantees to Users, either express or implied with respect to the Springer nature journal content and all parties disclaim and waive any implied warranties or warranties imposed by law, including merchantability or fitness for any particular purpose.
Please note that these rights do not automatically extend to content, data or other material published by Springer Nature that may be licensed from third parties.
If you would like to use or distribute our Springer Nature journal content to a wider audience or on a regular basis or in any other manner not expressly permitted by these Terms, please contact Springer Nature at

onlineservice@springernature.com